Higher Than Nyquist Test Waveform Synthesis and Digital Phase Noise Injection Using Time-Interleaved Mixed-Mode Data Converters

Xian Wang[1], Hyun Woo Choi[2], Thomas Moon[1], Nicholas Tzou[1] and Abhijit Chatterjee[1]
[1]Georgia Institute of Technology
[2]SAMSUNG Group

Abstract—In this paper, a higher than Nyquist RF test waveform synthesizer with digital phase noise injection is proposed. The proposed system uses time-interleaved digital-to-analog converters (DACs) and associated digital signal processing algorithms to enhance the spectral image of the synthesized waveform in the high-order Nyquist zones by increasing the effective sampling rate and eliminating unwanted signals inside the bandwidth of interest. The generated spectral images are used as the primary output of the proposed system. The waveform synthesizer is capable of digitally controlling the phase noise characteristics of the output signal in the high-order Nyquist zones. In addition, it utilizes relatively low-cost off-the-shelf integrated circuits (ICs) for multi-GHz signal generation. In hardware validation, dual DACs operating at 2.5Gb/s (effective Nyquist rate of 5 Gb/s) are used to generate a signal centered at 3.2GHz (corresponding to a Nyquist rate of 6.4 GHz). In addition, controlled phase noise generation is demonstrated.

Keywords- waveform synthesis; digital-to-analog conversion; sub-Nyquist rate; jitter injection

I. INTRODUCTION

The cost and complexity of testing equipment continues to increase as more complex high-speed and high precision consumer products are manufactured for the marketplace. In advanced high speed communication networks, timing and signal noise are critical parameters that limit system level performance. To resolve this, a low cost and high speed jitter immunity test with a test pattern that is capable of injecting different jitter characteristics is necessary [1]. In prior research, diverse mechanisms for jitter injection have been studied. These include modulating either the output buffer voltage or reference clock [2-3], using an arbitrary waveform generator (AWG) with pre-stored jitter, and a timing set from Automated Test Equipment (ATE) [4]. However, these methods have several limitations. These jitter modulation techniques are effective for periodic and random jitter injection but synchronization between the injected jitter and the applied test signal is difficult because jitter generation is generally decoupled from test pattern application. In addition, conventional AWG-based jitter injection is able to generate different kinds of jitter characteristics but its speed is limited by the sampling rate of the digital circuit and is not scalable to very high speed signals. The timing set function of automatic test equipment (ATE) facilitates on-the-fly jitter characteristic modulation, but lacks flexibility, since timing set resources within the ATE are limited [5].

Since AWG based jitter injection is more flexible across different injected jitter types, significant research has been performed in the past on increasing the effective Nyquist rate of the generated test signal without using very high speed digital-to-analog converters (DACs). Theoretically, N-parallel DACs can increase the effective Nyquist rate up to N times the sampling frequency of each individual DAC [6].

In this paper, a new time interleaved test waveform synthesis method is proposed. To generate a signal higher in frequency than the effective Nyquist rate, a high-order image replica in the frequency domain is filtered and used as the synthesized test waveform. Digital signal processing techniques are used to enhance the signal power of the image replica while suppressing unwanted signals within the signal bandwidth of interest, thereby reducing the in-band noise floor.

The key problem is to determine what data to feed into two interleaved DACs at lower frequency (called the baseband frequency) so as to produce the desired test signal at the higher frequency obtained by bandpass filtering the 1st or the 2nd image replica of the data fed to the DACs at the baseband frequency. Further, we desire to introduce noise into the baseband data so that the desired jitter statistics are obtained at the higher frequency corresponding to the synthesized waveform (image replica). To achieve this, a matrix model of the data transformation that occurs between the data fed into the two interleaved DACs and the resulting image replica is developed. This model combines several concepts: (a) frequency translation from the frequency of the baseband data to the frequency of the image replica, (b) a model for combining the responses of each of the two interleaved

DACs and (c) a model for the bandpass filter used to isolate the image replica from the system response. This is refered to as "in-band noise shaping" in the rest of this discussion. Through the use of a "pseudo inverse" on the whole matrix model, the best linear approximation to the target waveform is determined. Note that the image replica carries the same jitter characteristics of the baseband signal allowing a high speed signal (the image replica of the baseband/fundamental signal) with precise jitter characteristics to be obtained. Finally, an external bandpass filter is used to remove out-of-band noise.

The following section describes fundamental ideas and gives the system overview. The operation mode of the DAC used in this work is critical to the proposed waveform synthesis approach and is discussed next (section II.B). After that, Section III.B discusses the construction of the matrix models for test signal synthesis and filtering. Sections III.A, B describe the SNR optimization and signal synthesis algorithm formulation. Section III.C explains the use of the "pseudo inverse" for baseband signal determination. Section III.D discusses the function of the filter matrix for in-band noise shaping. Simulation results are presented in Section IV. Section V presents experimental results followed by conclusions in Section VI.

II. FUNDAMENTALS AND PROBLEM DEFINITION

A. Sampling Image Replicas

Any DAC receives discrete-time signal samples $x[n]$ as input at intervals of time T and generates as output, a continuous-time signal by convolving the samples with an output reconstruction filter. The reconstruction filter of a conventional zero-order hold (ZOH) DAC is modeled using a rectangular function.

$$x_{ZOH}(t) = \sum_{n=-\infty}^{+\infty} x[n] \cdot rect(\frac{t-T/2-nT}{T}), \qquad (1)$$

where $x[n]$ denotes the DAC input discrete-time signal, $rect()$ is the rectangular function [7], T the sampling period, $x_{ZOH}(t)$ the ZOH DAC continuous-time output signal. The effective impulse response of the zero-order hold system is given by

$$h_{ZOH}(t) = \frac{1}{T} rect(\frac{t-T/2}{T}), \qquad (2)$$

and its effective frequency domain response is

$$H_{ZOH}(j\omega) = \frac{2\sin(\omega T/2)}{\omega} e^{-j\omega T}, \qquad (3)$$

The Fourier transform of (1) is:

$$X_{ZOH}(j\omega) = \frac{1}{T} \sum_{n=-\infty}^{+\infty} X_B(j(\omega - \frac{2\pi n}{T})) \cdot H_{ZOH}(j\omega), \qquad (4)$$

where $X_B(j\omega)$ is the digital baseband spectrum. This equation indicates that, identical image replicas of $X_B(f)$ appear at multiples of ω. The change on spectrum is also presented in Fig. 1 below.
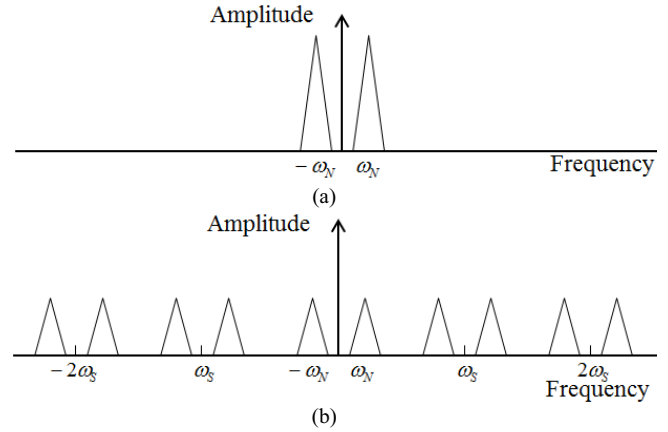

Figure 1. Spectrum of (a) $X_B(j\omega)$ (b) $X_{ZOH}(j\omega)$

The zero-order hold filter produces a sinc frequency response as shown in Fig. 2. As (4) indicates, all image replicas have the same information as the original signal but with lower power. There are mainly two reasons why a bandpass filter is not used in practice to isolate an image replica at a higher frequency. Due to the lower power of the image replica, the SNR of the extracted image is lower. Second, a narrowband bandpass filter with sharp cutoff is required for accurate image isolation. In the proposed signal synthesis approach, a high SNR value for the image replica is achieved by: (a) noise shaping and (b) cancellation of harmonics within the passband of the bandpass filter using special "modes" of operation of the DAC. The latter simplifies the design of the bandpass filter while allowing the target SNR value for the image replica to be achieved with ease.

B. DAC Operation Modes

In this section, the frequency responses of three DAC operation modes are discussed. As mentioned in the previous section, a conventional ZOH DAC operates by convolving the discrete time input samples with a zero-order-hold filter. The resulting spectral characteristic is shown in Fig. 2.
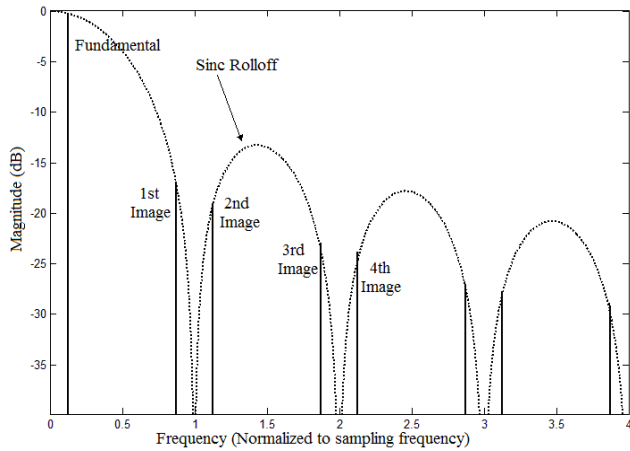
Figure 2. Reconstructed Spectrum with a zero-order-hold reconstruction filter

The descriptions used in the above image are defined in [8]. As mentioned before, the sinc roll-off shape should be taken into consideration whenever the image spectrum is used for direct waveform generation since the signal image suffers attenuation. The DACs used in the proposed method have three different kinds of output reconstruction mechanism as listed in Fig. 3: (a) normal mode, (b) return zero mode and (c) mixed mode.
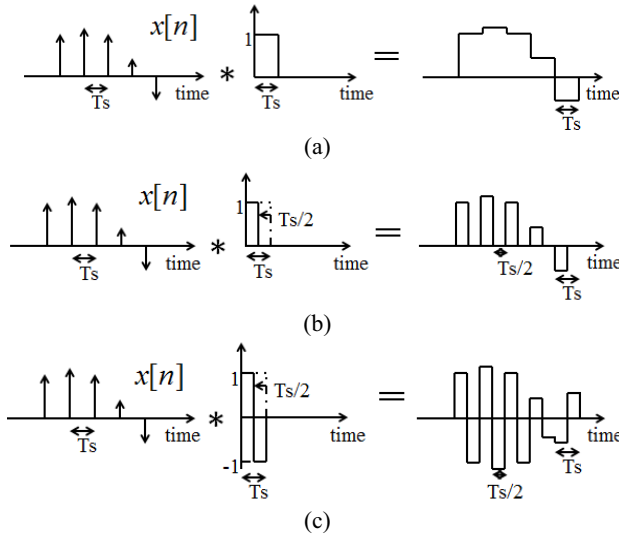

Figure 3. Convolution of a discrete data with reconstruction filter in (a) Normal Mode, (b) Return Zero Mode, and (c) Mixed Mode

As shown in Fig. 3, the normal mode of operation produces a step approximation to the digitized input signal. The return zero mode of operation produces an amplitude modulated pulse train response to the input

signal. The mixed mode of operation produces both a positive and negative going amplitude modulated pulse train response to the input signal. The reconstruction filter impulse responses for the return-to-zero mode and the mixed-mode are respectively shown below:

Normal Mode:

$$H(j\omega) = \frac{2\sin(\omega Ts/2)}{\omega} e^{-j\omega Ts/2} \tag{5}$$

Return-to-Zero Mode:

$$H(j\omega) = \frac{\sin(\omega Ts/4)}{\omega} e^{-j\omega Ts/4} \tag{6}$$

Mixed Mode:

$$H(j\omega) = \frac{\sin(\omega Ts/4)}{\omega} e^{-j\omega Ts/4} + \frac{\sin(\omega Ts/4)}{\omega} e^{-j\omega 3Ts/4} \tag{7}$$

The envelopes corresponding to each of the three different modes can therefore be calculated and are shown in Fig. 4.

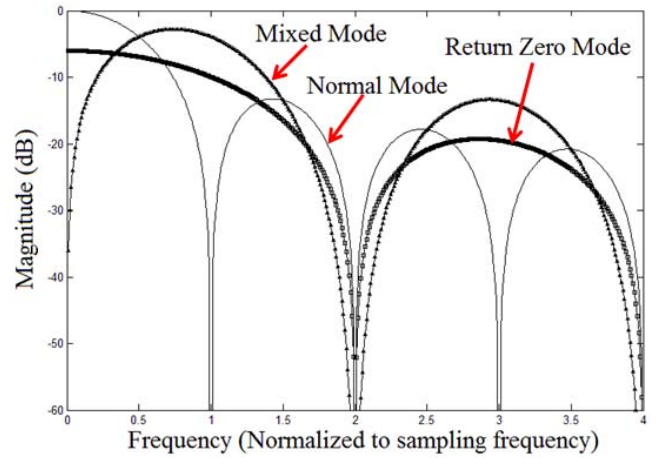Figure 4. Spectrum envelope of three different modes of DAC

Associating this figure with the locations of image replicas as shown in Fig. 2, the mixed mode operation of the DAC provided less attenuation of the 1st and 2nd images of the input signal. Therefore, DACs are operated in mixed mode in this paper in order to reduce the attenuation on image replicas.

III.   PROPOSED TEST SIGNAL SYNTHESIS
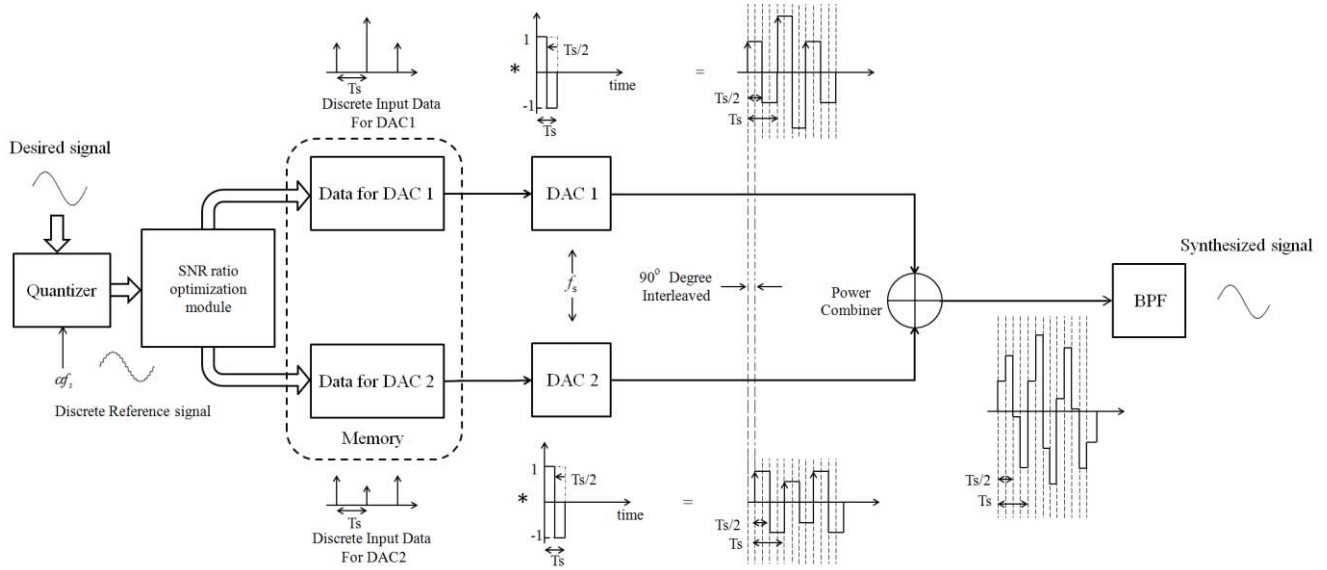
A.   System Overview

Figure 5. Graphical presentation of the technique

Fig. 5 shows an overview of the proposed higher than Nyquist signal synthesis technique. A high-precision discrete reference signal is digitally computed and generated using a direct digital synthesis (DDS) algorithm that uses very fine bit resolution, much higher than the bit resolution of the DAC hardware being used. This discrete reference signal consists of digital samples at a sampling rate of Nf_s, where N is the power of two, f_s is the DAC sampling speed. The reference signal is then fed to the signal-to-noise ratio optimization module to determine the individual, optimal input sequences of the multiple time-interleaved DACs (two DACs used in this research). The given input sequences are converted to analog signals by the DACs in a time-interleaved (90-degree phase offset), mixed-mode manner, and the generated analog signals are combined (added) using a RF power combiner. The transient waveforms at the power combiner inputs and output are illustrated in Fig. 5 as well. The combined signal is then fed through a band-pass filter if necessary to select a particular band under interest (higher than the Nyquist frequency).

B. Signal-to-Noise Ratio Optimization

The SNR optimization module receives a high-precision discrete reference signal as input and generates optimized data sequences as output to be fed to the time-interleaved DACs. Using the proposed algorithm, the output data sequences are optimized in the sense that the output signal of time-interleaved DACs controlled by the optimized bit sequences is corresponds to a least-squares fit of the high-precision input reference signal within the

frequency band of interest.

The high-precision reference signal is generated by using computer simulation including high bit-resolution DDS algorithms and signal modulation algorithms for a single-tone or multi-tone sinewave signals with amplitude/phase modulation. While one can use the proposed optimization technique to generate different types of signals, we conclude primarily the generation of single and multi-tone signals in this paper. The high-precision discrete reference signal $x_{ref}[\cdot]$ is given by

$$x_{ref}[k] = \sum_{m=1}^{\beta} A_m\left(\frac{k}{\alpha \cdot f_s}\right) \cdot \sin\left(2\pi f_{c,m}\frac{k}{\alpha \cdot f_s} + \phi_m\left(\frac{k}{\alpha \cdot f_s}\right)\right),$$
$$k = 1, 2, ..., 2^N, \tag{8}$$

where $f_{c,m}$ denotes the frequency of the test signal to be generated, f_s the DAC sampling speed, α the reference signal oversampling factor ($\alpha = 4$ is used in this paper), β the number of test tones, 2^N the number of samples in the reference signal $x_{ref}[\cdot]$ where N is an integer. $A_m(\cdot)$ and $\phi_m(\cdot)$ respectively denote the amplitude and phase modulation functions of the test signal. Optionally the selection of test signal frequency $f_{c,m}$ can be limited by the equation below to ensure the sampling coherency of the discrete reference signal.

$$\frac{f_{c,m}}{\alpha \cdot f_s} = \frac{\lambda}{2^N} \quad \lambda = 1, 2, ..., N. \tag{9}$$

Figure 6. Relation between matrix model and its I/O values

The SNR optimization algorithm outputs, or the input data sequences of the two DACs (DAC$_1$ and DAC$_2$) are respectively given by $\vec{x}_1^T = \{x_1[1], x_1[2], ... x_1[N/\alpha]\}$ and $\vec{x}_2^T = \{x_2[1], x_2[2], ..., x_2[N/\alpha]\}$. Note that these data sequences contain properly quantized values so that they can be fed to the low bit-resolution DACs as input. The output signals of DAC$_1$ and DAC$_2$ (time-interleaved) are denoted by $\vec{y}_1$ and $\vec{y}_2$ respectively, and the combined (or added) output signal $\vec{y}_{out}$ is modeled as shown below.

$$\vec{y}_{out} = [\vec{y}_1 + \vec{y}_2] = [H_1 \quad H_2]\begin{bmatrix} \vec{x}_1 \\ \vec{x}_2 \end{bmatrix} = H_{combined}\vec{x}_{input} \quad (10)$$

where $\mathbf{H_1} = [h^1_{i,j}]_{N \times N/\alpha}$ and $\mathbf{H_2} = [h^2_{i,j}]_{N \times N/\alpha}$ are the mixed-mode, time-interleaved DAC reconstruction filter matrix models for DAC$_1$ and DAC$_2$ respectively. The reconstruction filters are defined by

$$h^1_{i,j} = \begin{cases} 1 & i - \alpha(j-1) = 1 \; or \; 2 \\ -1 & i - \alpha(j-1) = 3 \; or \; 4, \\ 0 & otherwise \end{cases} \quad (11)$$

$$h^2_{i,j} = \begin{cases} 1 & i - \alpha(j-1) = 2 \; or \; 3 \\ -1 & i - \alpha(j-1) = 4, 5 \; or \; 1-N+\alpha, \\ 0 & otherwise \end{cases} \quad (12)$$

Fig. 6 shows the relationship between input data sequence of the DAC $\vec{x}_n$, discrete output signal $\vec{y}_n$ and DAC reconstruction filter matrix $\mathbf{H_n}$ (where n is either "1" or "2"). $x_{DAC}(t)$ is the time domain waveform generated by DAC.

For simplicity, $\mathbf{H_1}$ and $\mathbf{H_2}$ are given below when the reference signal oversampling factor $\alpha = 4$.

$$H_1 = \begin{bmatrix} 1 & & & \\ 1 & & & \\ -1 & & & \\ -1 & & & \\ & 1 & & \\ & 1 & & \\ & -1 & & \\ & -1 & & \\ & & \ddots & \\ & & & 1 \\ & & & 1 \\ & & & -1 \\ & & & -1 \end{bmatrix}, H_2 = \begin{bmatrix} & & & -1 \\ 1 & & & \\ 1 & & & \\ -1 & & & \\ -1 & & & \\ & 1 & & \\ & 1 & & \\ & -1 & & \\ & -1 & & \\ & & \ddots & \\ & & & 1 \\ & & & 1 \\ & & & -1 \end{bmatrix}. \quad (13)$$

Notice that 1 and -1 in the reconstruction filter matrix respectively represent normal sampling and inverse sampling in the mixed-mode operation of DACs, and that the location shift of matrix elements in $\mathbf{H_2}$ as compared with $\mathbf{H_1}$ represents the time-interleaved sampling (90-degree phase offset of sampling clocks) between DAC$_1$ and DAC$_2$. The proposed SNR optimization algorithm minimizes the error between the high-precision reference signal $\vec{x}_{ref}$ and the discrete-model of the system output signal $\vec{y}_{out}$ by using least squares minimization.

C. Least Squares Optimization

Given $H_{combined} \in \Re^{m \times n}$, the linear system formed by (10) consists m equations and n variables. When $m > n$, the system is known to be the over determined system. $\vec{x}_{input} \in \Re^n$ will be the solution of [9, 10]:

$$H_{combined}{}^T H_{combined} \vec{x}_{input} = H_{combined}{}^T \vec{y}_{out} \quad (14)$$

where $H_{combined}{}^T H_{combined} \in \Re^{n \times n}$ and $H_{combined}{}^T \vec{y}_{out} \in \Re^n$. (14) reduced equation number of the linear system from m to n. The solution of equation (10) is given as:

$$\vec{x}_{input} = (H_{combined}{}^T H_{combined})^{-1} H_{combined}{}^T \vec{y}_{out} \quad (15)$$

However, in this case, $H_{combined}{}^T H_{combined}$ is not a full column rank matrix, which makes $(H_{combined}{}^T H_{combined})^{-1}$ does not exist. Therefore, matrix decomposition techniques such as SVD, Cholesky decomposition, and QR[11], are used for approximating

$$H^+ \approx (H_{combined}{}^T H_{combined})^{-1} H_{combined}{}^T \quad (16)$$

where H^+ is called Moore-Penrose Pseudo inverse matrix[12]. For instance, when SVD decomposition is used $H_{combined} \in \Re^{m \times n}$ will be decomposed as:

$$H_{combined} = U \Sigma V^T \quad (17)$$

where $U \in \Re^{m \times m}$ and $V \in \Re^{n \times n}$ are orthonormal matrices and $\Sigma \in \Re^{m \times n}$ is the diagonal matrix. The Moore-Penrose Pseudo inverse matrix of $H_{combined}$ will be given as:

$$H^+ = V \Sigma^{-1} U^T \quad (18)$$

The inverse matrix is aiming at minimizing the error presented by:

$$\| H_{combined}(H^+ \vec{y}_{out}) - \vec{y}_{out} \| \quad (19)$$

where $\|.\|$ denotes the m dimensional Euclidean norm. And H^+ can be found through calling *pinv()* function in MATLAB

D. In-band Noise Shaping

The proposed in-band noise shaping algorithm is an extension of the SNR optimization algorithm described in Section III-B. This method is necessary especially when the high-precision reference signal cannot be generated coherently and the synthesized signal suffers from sampling incoherency induced distortions.

The purpose of the noise-shaping filter matrix H_{filter} is to make the SNR optimization algorithm focus on a particular frequency band so that noise and distortion caused by sampling incoherency or quantization errors is reduced within the band being defined. However, the wider the band, the higher the in-band noise floor is. The noise-shaping filter matrix is given by

$$H_{filter} = D^{-1} F D \quad (20)$$

where $\mathbf{D} = [d_{j,k}]_{N \times N}$ is the discrete Fourier transform (DFT) matrix, $\mathbf{D}^{-1}$ the inverse DFT matrix, and $\mathbf{F}$ is a diagonal matrix. The DFT matrix $\mathbf{D}$ is defined as [12]

$$D_{j,k} = (\frac{\omega^{(j-1)(k-1)}}{\sqrt{L}}) \quad (21)$$

where $\omega = e^{-\frac{2\pi i}{L}}$ in which $i = \sqrt{-1}$. The filter characteristic matrix $\mathbf{F}$ defines the frequency band of interest (or in-band) where the test signal is located. When the band of interest is defined as $[f_1, f_2]$ where f_2 is larger than f_1, $\mathbf{F}$ is given as shown below.

$$F_{i,i} = \begin{cases} 1 & \dfrac{f_1 N}{\alpha f_s} < i < \dfrac{f_2 N}{\alpha f_s} \\ 0 & i \in other value \end{cases} \quad (22)$$

The revised SNR optimization matrix model with the filter characterization matrix $\mathbf{F}$ is given by

$$H_{filter} H_{combined} \vec{x}_{input} = H_{total} \vec{x}_{input} = \vec{y}_{out} \quad (23)$$

where $\mathbf{H}_{total} = \mathbf{H}_{filter} \cdot \mathbf{H}_{combined}$. The least-square optimization algorithm described in Section III.B is used to generate the pseudo-inverse of $\mathbf{H}_{total}$ in order to obtain the optimal input data vector $\vec{x}_{input}$ and to generate an analog test signal with in-band noise reduction.

IV. SIMULATION RESULTS

A. Coherent Signal Generation

The SNR optimization algorithm described in Section III-B was tested in numerical simulation without using the in-band noise shaping technique. In the simulation, we implemented two mixed-mode DACs with a sampling rate of 2.5GSPS and a resolution of 8 bits. The high-precision reference signal was generated with a resolution of 32 bits and 2^{16} samples. For testing
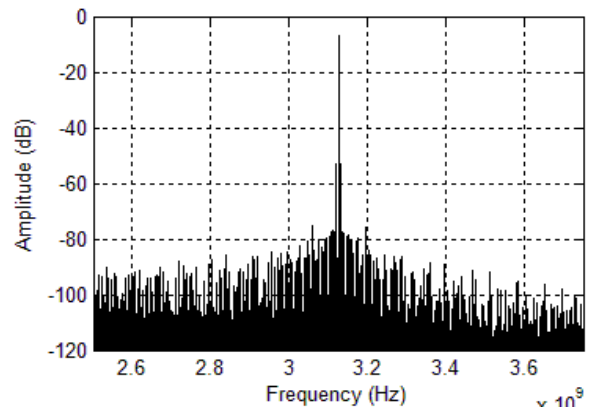
(a) Proposed Generating Method
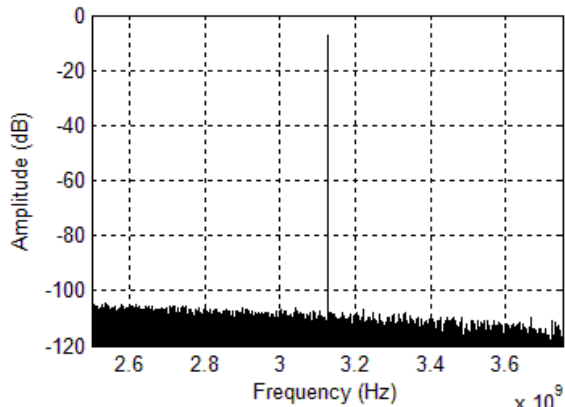
(a) Proposed Generating Method

(b) Conventional DDS Method
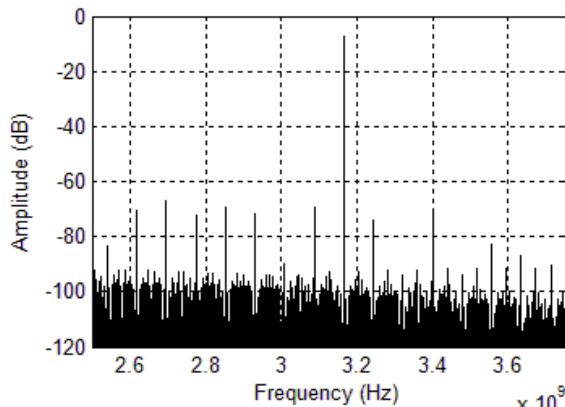
(b) Conventional DDS Method

Figure 7. Coherent sine wave generation

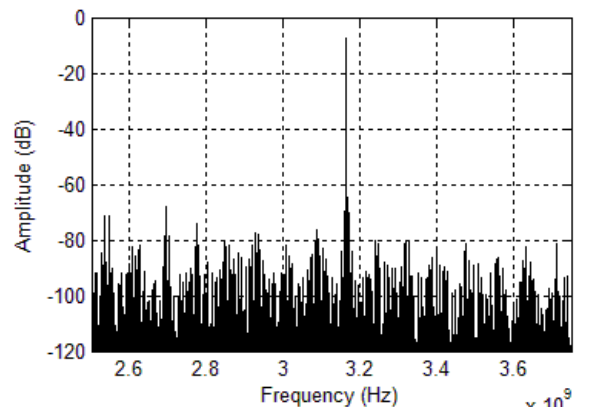Fig. 8 Coherent sine wave generation (with 5MHz jitter)

purpose, we used a single-tone reference signal with a center frequency of 3.125GHz but without amplitude/phase modulation, which corresponds to the 3rd Nyquist zone as defined in [8].

Fig. 7(a) shows the output spectrum of the time-interleaved, mixed-mode DACs with the proposed SNR optimization algorithm and Fig. 7(b) shows the one with a conventional DDS algorithm. It is noticeable that the noise floor and spurious distortion of the spectrum in Fig. 7(a) is less than those in Fig. 7(b). This is because the proposed algorithm reduces the output noise and distortion induced by non-ideality of DAC hardware including quantization errors. The proposed method helps the signal generator output a clean waveform with less harmonic and spurious distortions (or enhanced spurious-free dynamic range).

In addition with the single-tone signal generation, we performed jitter injection to the signal being generated.

Fig. 8(a) shows the output spectrum of a 3.125GHz signal with 5MHz sinusoidal phase noise (or jitter) injection generated by using the proposed SNR optimization algorithm, and Fig. 8(b) shows the one with the same signal parameters generated by using a conventional DDS algorithm. Notice that jitter injection to a particular tone being generated causes jitter of spurious distortion tones or other frequency components harmonically related with the tone being generated. For this reason, Fig. 8(b) shows combined spectra that consist of many tones (including the signal being generated) with their injected jitter sidebands. In comparison, the proposed method eliminates harmonic tones and spurious distortion in a target bandwidth. Therefore, the jitter sideband of the spectrum is clearly shown in Fig. 8(a).
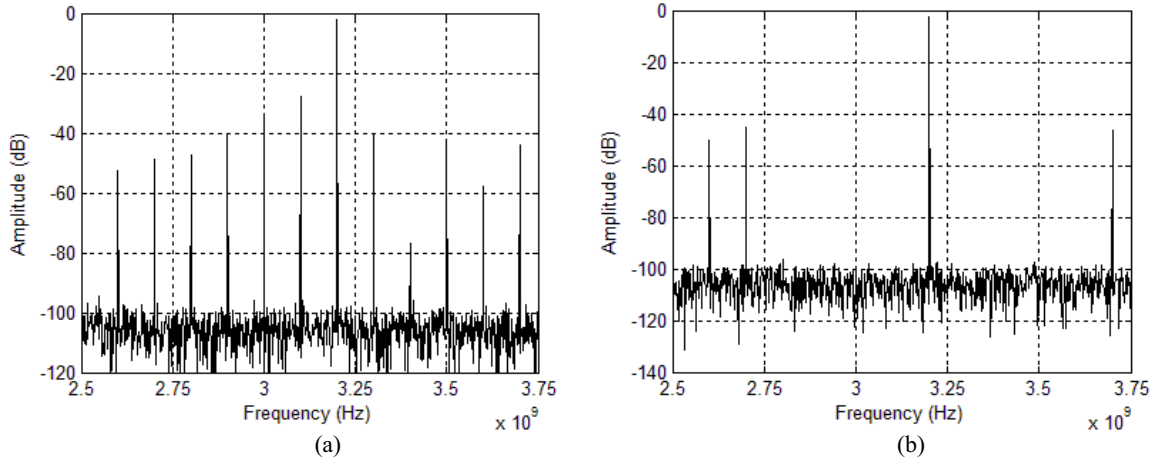
B. *Non-coherent Signal Generation*

Figure 9. Non-coherent pseudo-inverse generation (a) without filter matrix, (b) with filter matrix

When (9) is not satisfied, the DAC matrix model is non-coherent. With such a matrix model, the optimized value will have lots of distortions caused by non-coherency. This issue is minimized through applying the filter matrix described in Section III-C. Fig. 9 compares the waveform generation with/without filter matrix. The improvement is obvious.

V. MEASUREMENT RESULTS

A circuit prototype was built to prove the validation of the algorithm proposed. The circuit is designed with two identical DACs with maximum sampling rate of 2.5Gbps. Fig. 10 presents the circuit layout. Clocks of two DACs are generated, synchronized and delayed through clock conditioner, PLLs and digital delay chips respectively. The clock conditioner generates two synchronized clocks

Figure 10. Layout of AWG Board

at 100MHz. PLLs are then used to convert these slow clocks to 2.5GHz. After that, the delay chips are added to calibrate interleaving time between two clocks. And two output branches of DACs are designed to be identical in order to reduce the complexity of calibration. However, two DACs may have a response difference in a certain range, a further calibration is also recommended.

Fig. 11 shows the experimental device step-up. Two external clock sources are used to generate interleaved clock for two DACs. A power combiner is connected to two DACs output to perform signal addition. The added signal is finally goes to spectrum analyzer for analysis.

A. Single Tone Generation

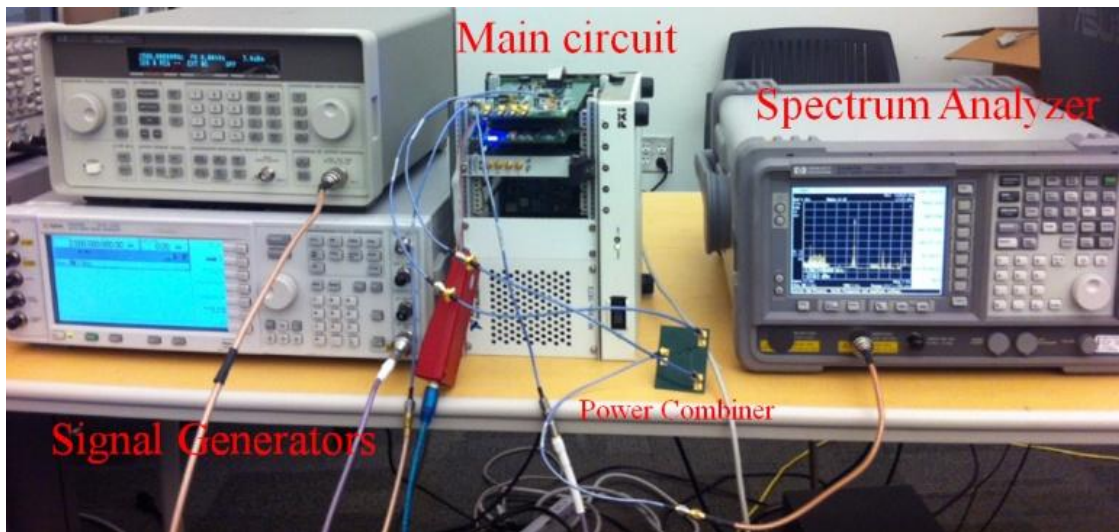Fig. 12 shows a single 3.2GHz sinusoidal waveform generated with an interested bandwidth from 2.8GHz to 3.6GHz.

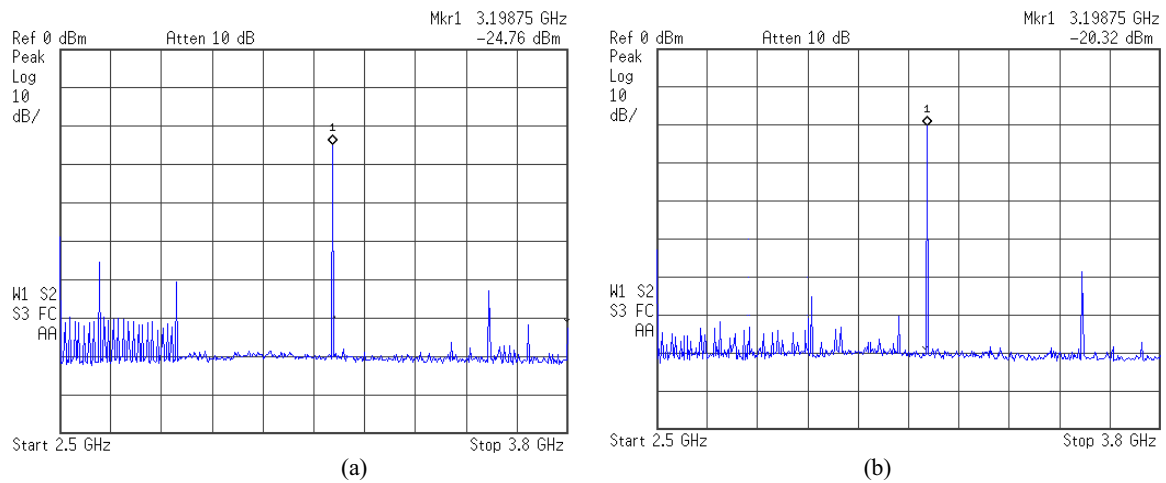Figure 11. Equipment Set-up

| (a) | (b) |

Figure 12. Single tone generation (8-bit) by (a) pseudo-inverse, (b) DDS

Measured signal value is lower than simulated one. This mainly caused by the long cable length and insertion loss of power combiner. When DDS is used, the low resolution results in an increase in noise floor and harmonic amplitude. The proposed method has shaped the noise out of interested band and obtained a clearer signal.

B. Jitter Injection

Fig. 13 and Fig. 14 show frequency spectra when the deterministic jitter is injected.

The peak to peak amplitude of the jitter is set to be 1ps and the frequency is 12MHz. Fig. 14 gives a closer look of the jitter injected signal. In Fig. 14, the jitter injection process neither increased the in-band noise floor nor increased the phase noise of the main tone. The harmonics of the injected jitter is observable and due to the envelope shape of reconstruction matrix, the harmonics of jitter is not symmetric.
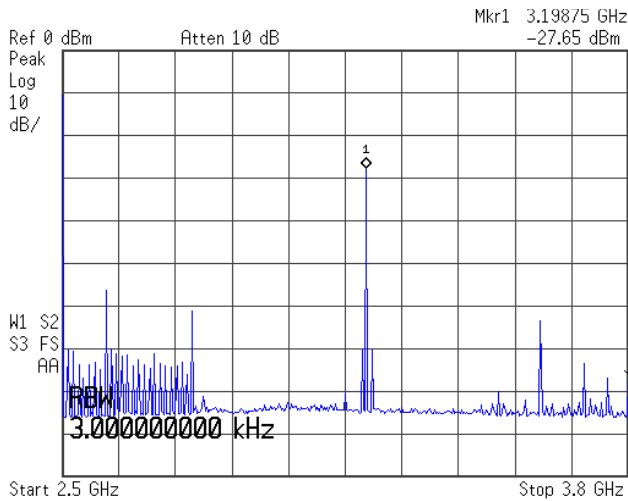
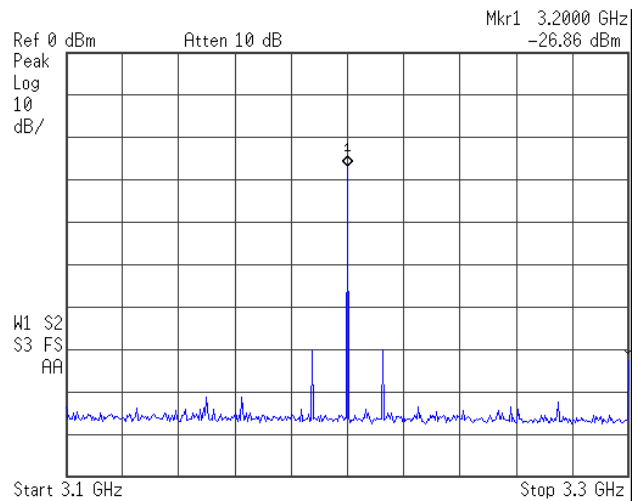Figure 13. 3.2GHz sine wave with 12MHz deterministic jitter injection

Figure 14. 3.2GHz sine wave with 12MHz deterministic jitter injection

VI. CONCLUSION AND FUTURE WORK

This paper extended jitter injection method based on AWG. Two DACs were used to perform a time-interleaved waveform reconstruction within a defined bandwidth. Simulation results have proved the conceptual validation of this method. And experiment results have given an evidence of it. In the experiment, the proposed algorithm is able to remove unwanted distortions and harmonics from interested band centered at a frequency that is higher than Nyquist rate of the DAC. Apart from that, it also shows the precise deterministic jitter injection is possible with proposed method.

By applying this technique, it is possible to generate high frequency jitter-injected signal with relatively lower cost. Practically speaking, the effect of this solution is limited by hardware similarities between two DACs. Further studies will be conduct on real time input data generation, model matrix coherency study and device calibration.

REFERENCES

[1] ITU-T O.171 (1997) Timing Jitter and Wander Measuring Equipment for Digital Systems which are based on the Plesiochronous Digital Hierarchy (PDH).

[2] D.C. Keezer, D. Minier, and P.Ducharme. "Variable Delay of Multi-Gigahertz Digital Signals for Deskew and Jitter-Injection Test Applications," Design, Automation and Test in Europe, pp. 1486-1491, Mar., 2008.

[3] Lucy Liu and Eddie Lew. "Periodic Jitter Amplitude Calibration with Walking Strobe" IEEE International Test Conference, pp. 1-8, Oct. 2006.

[4] M. Shimanouchi. "Periodic Jitter Injection with Direct Time Synthesis by SPP™ ATE for SerDes Jitter Tolerance Test in Production," IEEE International Test Conference, pp. 48-57, Oct., 2003.

[5] T.Fujibe, M.Suda, K.Yamamoto, Y.Nagata, K.Fujita, D.Watanabe, T.Okayasu. "Dynamic Arbitrary Jitter Injection Method For >6.5Gb/s SerDes Testing" IEEE International Test Conference, pp. 1-10, Nov. 2009.

[6] Stanley Yuan-Shih Chen, Nam-Seog Kim, and Jan M. Rabaey, "Multi-Mode Sub-Nyquist Rate Digital-to-Analog Conversion For Direct Waveform Synthesis," Signal Processing Systems IEEE Workshop. pp. 112-117, Oct. 2008.

[7] Bracewell, R. "Rectangle Function of Unit Height and Base, ." In The Fourier Transform and Its Applications. New York: McGraw-Hill, pp. 52-53, 1965.

[8] P. Hendriks, "Specifying communications DACs," IEEE Spectrum, vol.34, no.7, pp. 58-69, July 1997.

[9] G. Golub and C. van Van Loan, "Matrix Computations" (Johns Hopkins Studies in Mathematical Sciences), 3rd Edition, The Johns Hopkins University Press, 1996

[10] D. S. Watkins, "Fundamentals of matrix computations". Wiley; 3 edition, July 6, 2010.

[11] E. Anderson et al., LAPACK Users' Guide, Third.Philadelphia, PA: Society for Industrial and Applied Mathematics, 1999.

[12] P. Courrieu, "Fast computation of Moore-Penrose inverse matrices", in Neural Information Processing Letters and Reviews, 2005.